Polymer Degradation and Stability 106 (2014) 97–107

Contents lists available at ScienceDirect

Polymer Degradation and Stability

journal homepage: www.elsevier.com/locate/polydegstab

Towards a reference polyurethane foam and bench scale test for assessing smoldering in upholstered furniture

Mauro Zammarano [a,b,*], Szabolcs Matko [a], William M. Pitts [a], Douglas M. Fox [b], Rick D. Davis [a]

[a] Engineering Laboratory, National Institute of Standards and Technology, Gaithersburg, MD, USA
[b] Dept. Chemistry, American University, Washington DC, USA

ARTICLE INFO

Article history:
Received 3 October 2013
Accepted 8 December 2013
Available online 27 December 2013

Keywords:
Polyurethane
Foam
Smoldering
Upholstered furniture

ABSTRACT

Smoldering poses a severe fire hazard due to the potentially lethal amount of toxic carbon monoxide released, and the possible transition from smoldering to flaming (eventually leading to rapid fire growth and flash-over) with ignition sources otherwise too weak to directly induce flaming. Smoldering in residential-furniture upholstery materials can be assessed at a bench-scale by using reference materials with consistent smoldering behavior. However, the preparation of a reference foam has proven to be a challenging task, and the bench-scale tests currently in use may underestimate smoldering in actual furniture.

The aim of this work is to provide guidance for the selection/development of: (i) a reference flexible polyurethane foam with reproducible and well-characterized smoldering behavior, and; (ii) the development of a bench-scale smoldering test capable of identifying the upholstery materials (e.g., fabric, filling/padding, barrier, welt cord) that most likely prevent smoldering ignition in actual furniture.

In the first part of this paper, the impact of foam morphology on smoldering is discussed. It is shown how reticulated flexible polyurethane foams, possibly filled with carbon black, can be exploited as reference foam materials. Their fully open cell structure ensures consistent air permeability with an adjustable smoldering intensity as a function of their average cell size.

In the second part of this paper, a bench-scale smoldering test (currently employed in a number of test procedures and standards) is redesigned in such a way that the buoyant airflow within the foam is enhanced. Up to a three-fold increase in the rate of smoldering propagation and 400 °C increase in smoldering temperature is observed in the modified test as compared to the current tests. Transition to flaming was observed, only in the modified test, when an external enclosure was used. The modified test may offer a near-worst-case scenario, useful to identify the upholstery materials that prevent most smoldering ignitions independent of the construction and geometry of the actual furniture.

Published by Elsevier Ltd.

1. Introduction

Smoldering poses a serious fire hazard. A large number of residential fire deaths can be attributed to smoldering materials, such as flexible polyurethane foams (FPUFs), commonly found in upholstered furniture and bedding [1–4]. In the U.S., residential mattress flammability has been reduced by the introduction of a cigarette smoldering ignition test (16 CFR 1632) [5] in 1973, and an open flame test (16 CFR 1633) [6] in 2007, which requires a heat release rate less than 200 kW and a 15 MJ limit on heat evolved in the first 10 min [3]. A low peak heat release rate is usually achieved by wrapping the mattress with a barrier fabric [7]; smoldering ignition resistance is achieved by using a glass fiber fabric or a non-charring polymeric layer that melts and shrinks away from the ignition source (e.g., polyester fiber batting) [8]. The extension of such an approach to residential upholstered furniture (RUF) is not straightforward. Unlike mattresses, RUF manufacturers utilize a large variety of construction geometries and types of upholstery fabrics to satisfy highly diverse consumer tastes and demands [9].

Smoldering of upholstered furniture is a complex problem that varies based on the properties of the components (e.g., FPUF, fabric, fire barrier, fiber batting, welt cord, etc.), the layering sequence of the components and the geometry/construction configuration of the product. It follows that the possible combinations are almost

* Corresponding author. Engineering Laboratory, National Institute of Standards and Technology, Gaithersburg, MD, USA.
E-mail addresses: mzam@nist.gov, mauro.zammarano@nist.gov, zammarano@gmail.com (M. Zammarano).

0141-3910/$ – see front matter Published by Elsevier Ltd.
http://dx.doi.org/10.1016/j.polymdegradstab.2013.12.010

limitless and, thus, real-scale testing for assessing the smoldering propensity of RUF is not an economically viable solution [9,10]. As an alternative, bench-scale tests have been proposed to assess, classify and be used as a basis for regulating smoldering resistance of upholstery materials and resilient fillings [11–14].

This approach requires reference materials with well-characterized and reproducible smoldering behavior. For example, the assessment of the smoldering propensity of an upholstery fabric requires a reference cigarette ignition source and a reference FPUF. NIST SRM 1196 cigarettes [15] fulfill the first requirement, the ignition source, but a well-accepted standard FPUF is not used to date. The specified properties for FPUFs in existing test procedures are not sufficient to guarantee repeatable smoldering [16–18]. Up to now, the proposed standard TB117-2013 has possibly the strictest requirements for a reference FPUF [13]; however, it does not specify the type of FPUF (polyester versus polyether), average cell size, and a proper air permeability range. All these properties, as shown in our recent publications [18,19] and reiterated in this paper, are of paramount importance for smoldering in FPUFs and explain why the preparation of FPUFs with consistent smoldering has proven to be a challenging task.

The thermal degradation of FPUFs in air is the result of two competitive decomposition pathways: an oxidative decomposition pathway (promoted by an increase in oxygen availability and surface area) and a non-oxidative decomposition pathway (promoted by an increase in heating rate) [20,21]. The oxidative decomposition is an exothermic reaction which generates a charred foam-like residue with high surface area. The non-oxidative decomposition pathway is an endothermic pyrolytic reaction which generates a liquid tar (primarily polyol used to produce the FPUF) and causes a drastic reduction in surface area due to the collapse of the cellular structure [20,21]. Shifting the decomposition towards the oxidative pathway increases the heat release. The charred material left behind the smoldering front is subject to further oxidation. This is a strongly exothermic reaction that leads to a rapid temperature increase and, possibly, transition to flaming [22,23]. Generally, the rate of heat release due to smoldering increases when the oxygen supply is increased, for example, by a draft or buoyancy driven convective flow [4,20,24].

Air permeability is a measurement of airflow through a foam for a given sample thickness and pressure drop. A higher air permeability of the foam promotes faster airflow in buoyancy driven convective airflow (pressure drop and airflow are proportional in the laminar range) and a higher heat release rate [25]. Air permeability is determined by the morphology of the foam.

FPUFs are formed by an interconnected network of segments (struts) and thin membranes (windows). The struts form a three-dimensional polyhedral lattice; each polyhedron in the lattice is referred to as cell. Windows might be present, broken or absent on each face of a cell. The air permeability of a FPUF is a function of the number of windows, cell size and strut thickness.

The morphology of the foam plays a key role in oxygen transport within the foam. The air permeability can vary by a factor of 100 or more in FPUFs [19]. In closed cell foams (foams where all the cells are enclosed by windows), the oxygen supply is low (oxygen transport is controlled by diffusion through the windows) and smoldering is severely limited. In open cell foams (foam without cell windows), oxygen can freely diffuse between the cells and oxygen supply is also boosted by natural convection [26].

As mentioned, higher air permeability of the foam promotes a faster airflow in buoyancy-driven convective flow but not necessarily a higher rate of smoldering propagation. An increase in the average rate of the smoldering propagation rate is observed when the increase in air permeability is achieved by reducing the number of residual closed cells; otherwise, when the increase in air permeability is achieved by increasing the cell size, a reduction in the average rate of smoldering propagation rate is observed, even without a significant variation in density [18,19].

Ideally, a constant and homogeneous air permeability and cell size are desirable for consistent smoldering. Unfortunately, the morphology of a FPUF is never perfectly homogeneous, due, for example, to temperature gradients that develop during the foaming process. Also, inevitable variations in processing parameters (e.g., atmospheric temperature/humidity and dosing of the reagents) induce morphological variations between different foam batches [19].

Bench-scale tests have been proposed to assess, classify and to be used as a basis for regulating smoldering resistance of cover/barrier fabrics and resilient fillings for RUF [11–14]. In these tests, two pieces of FPUF are placed, one vertically and one horizontally, at right angles to one another, simulating the seat and back of a chair (Fig. 1). The two pieces of FPUFs are held in place by a wooden frame and are covered with upholstery material. The cigarette ignition source is placed along the crevice formed by the two pieces of foam (see Section 2.5). This general configuration with a wooden frame will be referred to as a "standard mockup" test. These types of tests are based on a "sectional approach", i.e., they aim to simulate the section of the RUF with the highest likelihood of smoldering ignition: the junction formed by a seat (horizontal) and back (vertical) cushions [10,16,27].

However, the standard mockup test might underestimate smoldering of certain RUFs, where the foam sits on an open substrate, such as springs. In such a configuration, the airflow generated by buoyancy-induced natural convection promotes smoldering by boosting the oxygen supply rate [25]. It is expected that this buoyant airflow is to a large extent suppressed in the standard mockup test, where a large fraction of the sample foam surface is in contact with solid wooden panels. Experimental results indicate that if the airflow becomes too slow, smoldering will self-extinguish, and conversely, if the airflow is rapid enough, then smoldering can transition to open flame [27].

Self-sustained smoldering, or simply sustained smoldering, occurs by definition when the smoldering front has extended to a region beyond the thermal influence of the ignition source. The U.S. Consumer Product Safety Commission [16] observed that some combinations of upholstery materials led to sustained smoldering (detected as continued production of smoke and heat after the extinguishment of the ignition source) in real-scale RUF mockups (where FPUF sits on springs rather than a wooden frame) and non-sustained smoldering in a standard mockup test configuration. This result shows that the standard mockup test, where the buoyant airflow is largely suppressed, can underestimate smoldering propensity under certain conditions. This is undesirable for a test meant to identify upholstery materials that are unlikely to develop sustained smoldering in RUF.

It would seem to be desirable to develop a small-scale test capable of more closely matching the real-scale RUF used in Ref. [16] and offering a near-worst-case mockup configuration so that variation from this scenario in actual furniture would most likely give less severe smoldering [10].

This study is divided into two parts and aims to provide guidance to address two potential shortcomings of standard mockup tests in the assessment of smoldering resistance of RUF materials: (i) the lack of a reference FPUF and (ii) the possible underestimation of smoldering propensity in the standard mockup. In the first part of this study, the performance of reticulated foams (fully open-cell FPUFs obtained by a chemical or thermal post-process which removes all the residual cell windows [28]) as reference materials for smoldering tests was investigated. In the second part of the study, the standard mockup test has been redesigned to enhance the convective airflow

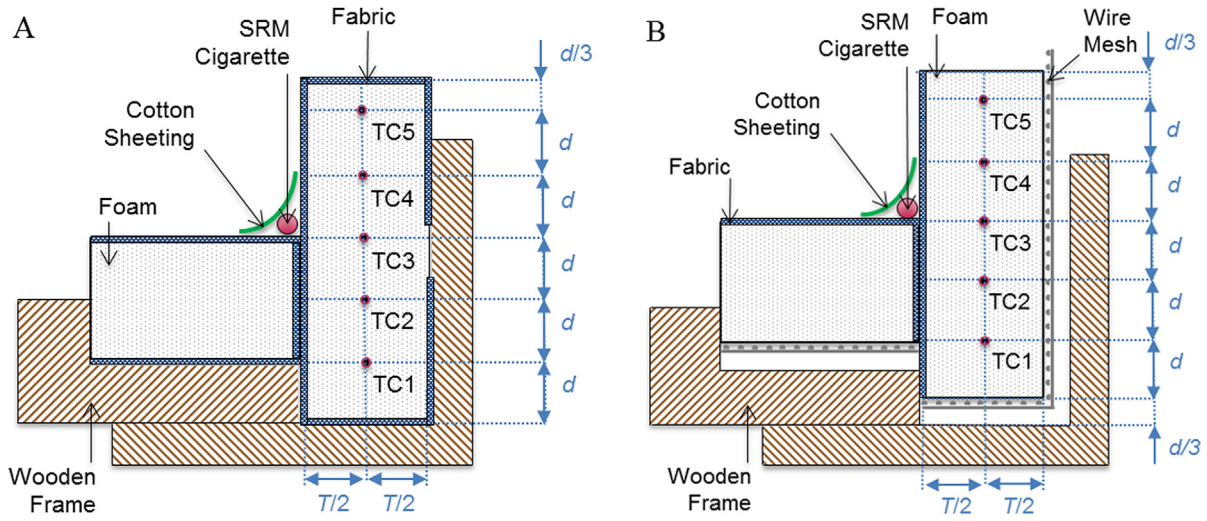

Fig. 1. Schematic drawing of the standard mockup test (A) versus the modified mockup test (B): a gap between the foam and the wooden frame and a partial removal of the upholstery fabric aim to promote natural convection in the modified mockup. Five thermocouples (TC1 to TC5) were installed in both configurations (d = 38 mm; T = 76 mm).

within the FPUF. The impact of such modification was investigated by comparing the smoldering behavior of three different types of FPUFs in the standard and modified mockup tests.

2. Experimental section[1]

Uncertainty is reported as two standard deviations (2σ) throughout the paper.

2.1. Materials

All materials were used as received unless otherwise indicated. Both custom-made and commercial FPUFs were used in this study. All FPUFs were based on toluene diisocyanate (TDI) (mass ratio mixture of 2,4- (80%) and 2,6-isomers (20%)). The custom-made foams (foam types 5 to 9 of Table 1) contained commercial-grade polyether triols with molar masses between (3000 and 3200) g mol^{-1} and OH numbers between (50.5 and 57.5) mg KOH g^{-1}. Similarly, commercial-grade organo/silicone surfactants for PUF were selected. The other reagents used were TDI, water, an amine based catalyst (DABCO 33LV, Airproducts), a polyether based catalyst (Niax C323, Momentive), a tin-catalyst (Kosmos 29, K29, Evonik) and a fatty ester emulsifier (Addotovate D1092, RheinChemie). As discussed elsewhere [19], the specific polyol and surfactant did not show any systematic significant effect on smoldering behavior and, for the sake of conciseness, are not further specified here. The commercial FPUFs of Table 1 were based on polyether polyols (foam type 1, 3, 4 and 10) or polyester polyols (foam type 2).[2] Foam type 10 contained about 0.5% by mass of carbon black. Foam types 1, 2, 3 and 10 were post-processed by reticulation.

2.2. Sample preparation

Custom foams were prepared by a foam manufacturer in a small pilot plant or on a production line. In both cases, all reagents were pumped at a controlled rate into a fixed mixing chamber (mixing head). The pressure in the mixing head was adjusted by controlling a valve at the outlet for a range of (35–124) kPa. In the pilot plant, the material was transferred from the mixing head to a foaming box through a feeding tube. After 15 min at room temperature, the foams were cured in an oven at 110 °C for 1 h and post-cured at room temperature for an additional 24 h. On the production line, the ingredients of the foam formulation were discharged through the nozzle of the mixing head and deposited onto the front of a conveyor belt; the temperature of the foam typically reached about

Table 1
Type of FPUF and values of air permeability (Φ), cell area (Σ) and char volume fraction in the standard mockup (CVF_{SM}). The number of replicate tests (n) is also reported. Uncertainty is reported as two standard deviations. See Sections 2.1 and 2.2 for details on chemical reagents and processing conditions used for each foam type.

FPUF type[a]		Air permeability		Cell area		Smoldering	
		Φ (m min^{-1})	Tests (n)	Σ (mm^2)	Tests (n)	CVF_{SM} (%)	Tests (n)
1	Ether, L, RT, C	≈78[c]	–	0.20 ± 0.02	4	82 ± 6	5
2	Ester, L, RT, C	82 ± 4	5	0.22 ± 0.01	4	8 ± 2	6
3	Ether, L, RT, C	87 ± 4	8	0.24 ± 0.01	4	69 ± 12	5
4	Ether, L, C	81 ± 2	5	0.29 ± 0.04	5	29 ± 8	5
5	Ether, S, NC	82 ± 12	5	0.33 ± 0.04	4	32 ± 6	5
6	Ether, L, NC	78 ± 22[b]	96	0.39 ± 0.03[b]	15	17 ± 16	47
7	Ether, S, NC	74 ± 16	5	0.57 ± 0.06	4	8 ± 6	4
8	Ether, S, NC	71 ± 22	5	0.60 ± 0.04	4	8 ± 8	4
9	Ether, S, NC	79 ± 14	5	0.62 ± 0.02	4	2 ± 4	4
10	Ether + CB, L, RT, C	184 ± 12[b]	60	0.69 ± 0.08[b]	16	20 ± 8	6

[a] FPUF type: Ether (polyether FPUF), Ether + CB (polyether FPUF filled with carbon black), Ester (polyester FPUF), L (large foam manufactured on a production line), S (small foam manufactured in a pilot plant), RT (post-processed by reticulation), C (commercial foam), NC (custom-made foam).
[b] These values of Φ and Σ were calculated with multiple measurements across an entire large FPUF; all other values were calculated on smaller FPUFs or in specific locations of large FPUFs.
[c] Value of Φ estimated from the values of Φ for foam types 2, 3 and 10 supposing a linear correlation between Σ and Φ in reticulated FPUFs.

[1] The policy of the National Institute of Standards and Technology (NIST) is to use metric units of measurement in all its publications, and to provide statements of uncertainty for all original measurements. In this document however, data from organizations outside NIST are shown, which may include measurements in non-metric units or measurements without uncertainty statements. Certain commercial entities, equipment, products, or materials are identified in this document in order to describe a procedure or concept adequately or to trace the history of the procedures and practices used. Such identification is not intended to imply recommendation, endorsement, or implication that the entities, products, materials, or equipment are necessarily the best available for the purpose. Opinions, interpretations, conclusions, and recommendations are those of the authors and are not necessarily endorsed by NIST.

[2] For the remainder of the paper, FPUFs based on TDI and polyether polyols, and FPUF based on TDI and polyester polyols will be referred to as polyether FPUF or polyester FPUF, respectively.

(150–170) °C; curing was completed in air, and no post-curing was required. Foams were produced in two different sizes: "large foams," manufactured in the production line with dimensions of 1.3 m (width) × 0.6 m (height) × 3 m (length in the pouring direction), and "small foams," manufactured in the pilot plant with dimensions of 0.5 m × 0.8 m × 0.3 m (height).

2.3. Cell size measurements

In general, three-dimensional imaging is required for cell size measurement, whereas two-dimensional imaging provide an "apparent" cell size that is a function of the optical-slice thickness. Here, for simplicity, the cell size was measured by two-dimensional imaging with constant optical thickness. Foam anisotropy and heterogeneity were assessed by imaging in orthogonal planes and different foam locations, respectively. The cell size was expressed in terms of average cross-sectional area of the cell, calculated by image analysis. The detailed procedure is described below.

A *z*-stack (sequence of images at increasing depths within the sample [29]) of 20 images from the FPUF surface was collected by scanning an area of (11.9 × 11.9) mm^2 with a confocal microscope (LSM 510 META Carl Zeiss, Germany) (5× magnification, 405 nm diode laser, 420 nm low-pass filter, 19.75 μm optical thickness per image). From each *z*-stack, the image that showed the highest average intensity was selected for image analysis (ImageJ, National Institutes of Health) [30], and processed as follows: (1) Gaussian filter blurring with a diameter of 20 pixels for noise removal; (2) local-maxima algorithm (noise tolerance: 2, output type: segmented particles) for identifying the contour of the cells; (3) ImageJ macro "analyze particle" for calculating the area of each segmented particle (i.e., cell) with proper cell filters (cell area above 0.02 mm^2, exclude particles on edge, circularity[3] equal to or above 0.75) for minimizing small artifacts (i.e., erroneous identification of nonexistent small cells), over-segmentation (i.e., erroneous identification of one cell as multiple cells) and under-segmentation (i.e., erroneous identification of multiple cells as one cell). The average value of cross-sectional area of the cell for a given *z*-stack (Σ_{stack}) was then calculated.

Foam anisotropy was assessed using cubic FPUF samples (side length of about 15 mm), scanning one *z*-stack for each of three selected orthogonal sides of the cube, and measuring Σ_{stack} for each of these sides (all cubic samples were cut from a larger sample of FPUF so that two opposite sides of the cube were parallel to the original bottom surface of the FPUF).

The local value of cell area (Σ_{local}) was calculated as the average of the three Σ_{stack} values of a cube. Σ_{local} identifies the cell area in a specific foam location. Σ_{local} values were measured in at least four locations per foam type.

The cell area for a FPUF (Σ) was calculated as the average of these Σ_{local} values. The uncertainty of Σ was expressed as $\pm 2\sigma$, where σ is the standard deviation of these Σ_{local} values. Thus, the reported Σ uncertainty increases with foam heterogeneity and is not affected by foam anisotropy.

2.4. Air permeability

The air permeability (Φ) is a measurement of the volume of air flowing per unit of time through a FPUF sample for a given thickness and area at a given differential pressure. A differential-pressure airflow tester (FAP 5352 F2, Frazier Instrument Co. Inc., Hagerstown, MD) was used in this study. Foam was cut into samples (90 × 90 × 13) mm^3 and placed in a circular clamp, exposing a surface of 38.5 cm^2 to a perpendicular airflow. The target pressure-drop through the 13 mm (1/2 inch) thick foam slice was set to 127 Pa (13 mm of water). This method, initially developed for textile fabrics, is currently used to measure airflow through polyurethane foams [31]. The tests were conducted at room temperature. The values of air permeability (Φ) are expressed in terms of volumetric airflow as cubic meters per square meter of sample per min (or simply meters per min) at a temperature of 0 °C and a pressure of 100 kPa. Air permeability was measured on foam slices parallel to the original bottom surface of the foam.

2.5. Smoldering

Smoldering was assessed by a standard test (referred to as "standard mockup"), inspired by existing smoldering ignition resistance tests [11–14], and by a modified test (referred to as "modified mockup"), described here. Fig. 1 shows schematic drawings of the standard mockup (A) and the modified mockup (B).

In both mockup configurations, two pieces of FPUF, one (203 × 203 × 76) mm^3 (vertical) and one (127 × 203 × 76) mm^3 (horizontal), were placed at right angles to one another, simulating the crevice formed by a seat and back of a chair. The surface of the foam to be tested was covered by an upholstery fabric. A lit cigarette (Standard Cigarette for Ignition Resistance Testing, NIST SRM 1196) [15] was placed in the crevice formed by the two foam pieces, and was then covered by a piece of a standard lightweight fabric, a 100% cotton, white plain weave of (19–33) threads/cm^2 and areal density of (115 ± 1) g m^{-2}. The test duration was 45 min. A cotton upholstery fabric with a consistently high smoldering tendency (100% cotton, indigo twill weave with an average aerial density of 445 g m^{-2} ± 3 g m^{-2}) was selected for this study and used with all foams. Five thermocouples (TC1 to TC5) (0.5 mm thick K-type thermocouples, KMQXL-020G-12, Omega Engineering Inc.) were installed on the center line of the vertical foam according to the pattern of Fig. 1. Temperature measurements were recorded at a sampling interval of 1 s.

The modified mockup differed from the standard mockup by the introduction of a 13 mm gap between the foam and the wooden frame and the removal of the upholstery fabric from the bottom, back and top of the mockup (see Fig. 1). The upholstery fabric covering the horizontal foam had dimensions of (330 × 203) mm^2 in the standard mockup and (203 × 203) mm^2 in the modified mockup. The upholstery fabric covering the vertical foam had a dimensions of (508 × 203) mm^2 in the standard mockup and (203 × 203) mm^2 in the modified mockup. The foam was supported above the wooden frame by a stainless-steel welded-wire mesh with a mesh size of about (6 × 6) mm^2 and a wire diameter of about 1 mm. This configuration promotes an increase in buoyant airflow through the FPUF.

At the end of the test, the charred foam was carefully removed, and the mass loss of the foam was calculated as the difference between the initial mass of the foam and the mass of the residual foam after char removal [11]. Assuming that the density of the virgin foam was homogeneous and did not vary during the smoldering test, the volume fraction percentage of foam converted into char by the end of the test (*CVF*) (for the remainder, in short, referred to as "char volume fraction") is equal to the mass loss percentage of the foam, and the average volumetric rate of the smoldering front during the test (*AVR*) (for the remainder referred to as "smoldering propagation rate") is equal to $CVF \times V_0/(100t)$, where $V_0 \approx 5091$ cm^3 is the initial volume of foam and $t = 45$ min is the test duration. It follows that $AVR = c \times CVF$, with $c \approx 1.13$ cm^3/min. Thus, *CVF* is proportional to *AVR*; *CVF* was used in this work to assess the smoldering propagation rate.

[3] Circularity of a cell is defined as $4\pi(A/P^2)$, where A and P are the area and the perimeter of the cell, respectively.

In a limited number of tests, the mass loss of the mockup (equal to the sum of the mass losses of the foam, fabric, cotton sheeting and ignition cigarette) was also recorded in real-time.

Non-sustained smoldering was identified by the absence of smoke and heat production after the complete combustion and self-extinguishment of the cigarette. Self-extinguishment of the ignition source typically occurred in less than 28 min.

The mockup tests were run inside a hood with inner dimensions of 165 cm (width) × 86 cm (depth) × 66 cm (height) and an open top allowing an air inflow lower than 0.6 m^3 min^{-1}. When indicated, each mockup was placed inside an enclosure to minimize airflow variations in the hood and suppress turbulence. The 53 cm (width) × 36 cm (depth) × 50 cm (height) enclosure had four holes (13 mm diameter) in proximity of the bottom corners and seven slits (280 mm × 13 mm) on the top side. All FPUF samples were conditioned at (21 ± 2) °C and (50–56) % relative humidity for at least 24 h prior to testing. The same environmental conditions were used during the smoldering tests.

3. Results and discussion

3.1. Impact of FPUF morphology on smoldering and reticulated foams

The morphology and smoldering propensity of 10 FPUF types are summarized in Table 1. The cellular morphology was characterized in terms of cell area (Σ) and air permeability (Φ); smoldering was evaluated in terms of char volume fraction measured in the standard mockup (CVF_{SM}), which is proportional to the smoldering propagation rate in the standard mockup (AVR_{SM}).

The densities of these foams were in the range of (23–34) kg m^{-3}. Density was not further considered in this study because it had no discernible effect on smoldering within the experimental parameter space investigated here [18].

The cell area values Σ in Table 1 were calculated by image analysis of confocal images. Fig. 2 shows a few examples of confocal images in which the contours of the cells, identified by image analysis, are highlighted (cyan lines). Not all cells are identified by the image analysis used here; this is an effect of the cell filters (see Section 2.3) applied to remove erroneously identified cells.

Due to foam anisotropy, the cell area measured in the horizontal plane (plane parallel to the original bottom surface of the foam) was (5–30) % smaller than the cell area in the vertical planes (any plane orthogonal to the horizontal plane), and the air permeability measured in a horizontal plane was about (20–30) % higher than the one measured in a vertical plane [19]. Thus, smoldering might be affected by anisotropy. In this work, for consistency, the mockup test samples were always cut from 76 mm-thick slices which were parallel to the horizontal plane.

All FPUFs in Table 1 had a largely open cell structure and relatively high air permeability (Φ > 70 m min^{-1}). For values of air

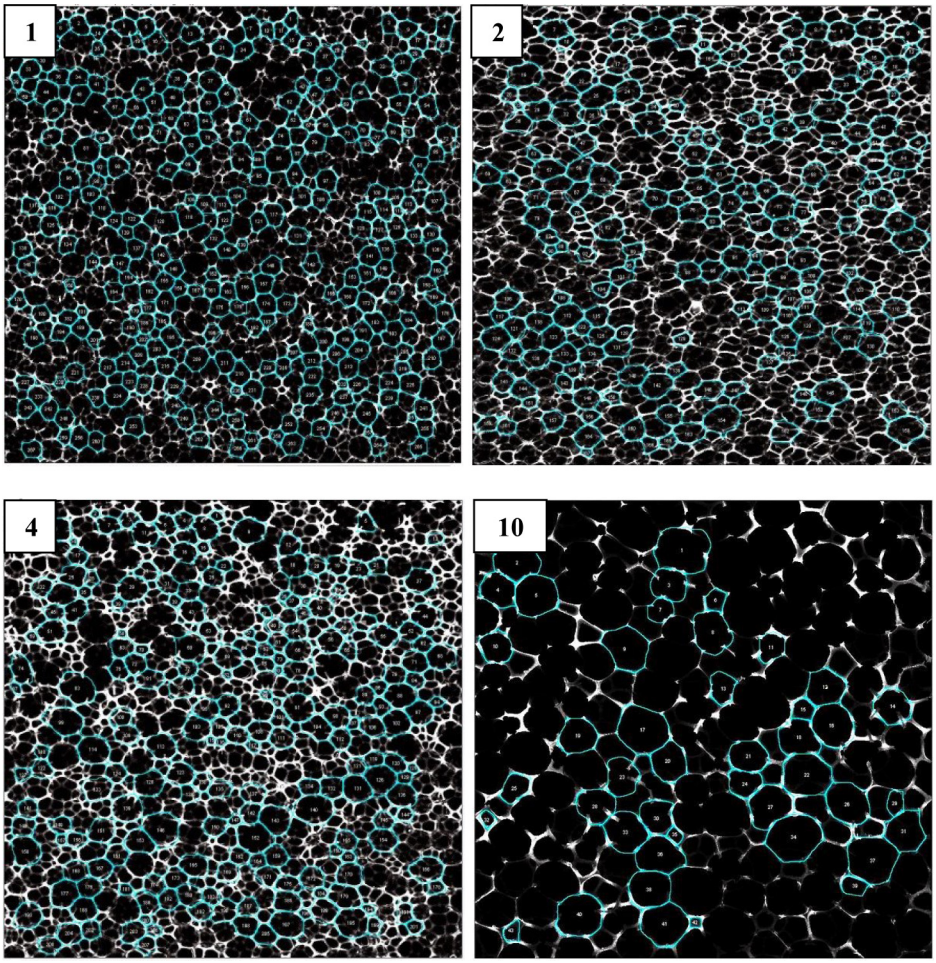

Fig. 2. Confocal images for foam types 1, 2, 4 and 10 showing the highlighted contours of the cells (cyan lines), identified by image analysis. All images were acquired from a plane parallel to the bottom original surface of the FPUF (image size: 11.9 mm × 11.9 mm). (For interpretation of the references to color in this figure legend, the reader is referred to the web version of this article.)

permeability below a threshold value ($\Phi_{threshold} \approx 50$ m min^{-1}), sustained smoldering was never observed in a standard mockup test with the upholstery fabric used here [18,19].

The values of char volume fraction in the standard mockup (CVF_{SM}) are plotted as a function of the values of cell area (Σ) in Fig. 3.

For polyether FPUFs, there is a clear correlation between Σ and CVF_{SM}, approximated by the following power-law regression fit (coefficient of determination $R^2 = 0.86$):

$$CVF_{SM} = 1.2\ \Sigma^{-2.8} \quad (1)$$

Note that Eq. (1) is valid for all polyether FPUFs of Table 1 which do not contain other additives (e.g., carbon black in foam type 10). It implies that, within the experimental parameter space investigated here, smoldering is not significantly affected by: the specific polyether polyol, surfactant and catalyst content/type; origin and processing of the foam. Some of these polyether FPUFs are custom made (foam types 5, 6, 7, 8, 9) and others are commercial grades (foam types 1, 3, 4). Some have been foamed in a pilot plant (foam types 5, 7, 8, 9) and others on a production line (foam types 1, 3, 4, 6). Some have been post-processed by reticulation (foam types 1, 3). Thus, Eq. (1) appears to be a surprisingly robust predictor for the smoldering propagation rate in polyether FPUFs, given that their air permeabilities Φ meet the requirement $\Phi > \Phi_{threshold}$.

For a given density of the FPUF, a smaller cell size induces a higher specific surface area of the foam (i.e., area available for oxidation) and a higher heat release rate due to a shift of the thermal degradation of FPUF from a pyrolytic to an oxidative pathway. In fact, the oxidation of the foam is a heterogeneous reaction and its rate is proportional to the specific surface area [32]. In general, the rate of smoldering propagation is determined by the balance between the rate of heat release in the reaction volume and the rate of heat loss from the reaction volume [20,22,24]; thus, the correlation between cell size and smoldering propagation rate, expressed by Eq. (1) ($CVF_{SM} \propto AVR_{SM}$), might be due to an increase in the oxidation rate with the specific surface area.

However, when smoldering is an oxygen limited reaction, the reaction kinetics have no effect on the rate of smoldering propagation because oxygen is completely consumed in the reaction volume [25,33,34]. This occurs when the airflow velocity within the foam is low. However, at higher airflow velocities (on the order of 1 mm/s), the smolder process becomes kinetically limited, and the smolder velocity is dependent on the rate of foam oxidation [33,34]. In this scenario, air travels too quickly through the reaction zone to allow a complete reaction of oxygen with the fuel. In an upholstered-type situation, the velocity of a self-generated buoyant airflow reaches values on the order of 1 mm/s where the kinetic parameters might play an important role [25].

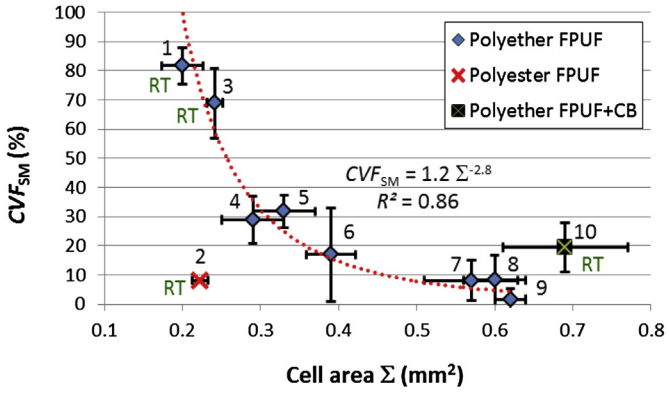

Fig. 3. Char volume fraction in the standard mockup (CVF_{SM}) versus cell area (Σ) for FPUFs having $\Phi > \Phi_{threshold}$. The diamond-shaped data points refer to polyether FPUFs (commercial and custom-made), some are post-processed by reticulation (RT); the dotted-line curve is a power-law least-squares regression fit to these data points (fitting equation and relative coefficient of determination R^2 shown). The data points for a polyester FPUF and a carbon-black-filled polyether FPUF are also reported. The uncertainties are shown as two standard deviations.

Another possible explanation for the observed dependance of CVF_{SM} over CVF_{SM} in an oxygen limited smoldering scenario is that, at larger values of cell size Σ, the slower oxygen consumption results in a thicker and lower-temperature smoldering wave. In this situation, the heat transfer to the virgin foam is lower, due to a smaller temperature gradient, and the smoldering propagation slows down [25].

The heat evolved by smoldering increases with air permeability in the laminar flow range, which is typical of buoyancy-induced natural convection in upholstery smoldering [25]. Eq. (1) does not take into account the effect of air permeability on smoldering, thus it is expected to be strictly valid for polyether FPUFs with air permeability about 80 m min^{-1}. In fact, Eq. (1) has been derived for FPUFs with Φ spanning the relatively tight range of (71–87) m min^{-1} (see Table 1). Standard polyether FPUFs used for RUF usually do not show air permeability much lower (due to the effect of air permeability on the viscoelastic response of the foam [35]) or higher than 80 m min^{-1} (due to residual cell windows and a relatively small cell size). Foam type 10 is the only one in Table 1 that shows an exceptionally high value of air permeability ($\Phi \approx 184$ m min^{-1}); this can be achieved with post-processing (reticulation) and a large cell structure ($\Sigma \approx 0.7$ mm^2) that are possibly used in specialty FPUFs, but not in common FPUF for RUF [19]. Foam type 10 has a value of CVF_{SM}, significantly higher than the one predicted by Eq. (1). Hence, the presence of a filler (about 0.5% by mass of carbon black) and/or the exceptionally high value of air permeability appear to boost smoldering rate.

Fig. 3 also displays results for one polyester FPUF (foam type 2). This foam is clearly an outlier with an approximately 10-fold decrease in CVF_{SM} value as compared to those predicted by Eq. (1). Reticulated polyether FPUFs with a comparable cell size and permeability (foam types 1 and 3) have much higher smoldering rates. This difference is likely due to the different polyols (i.e., polyester instead of polyether) used in the foaming process, resulting in different thermal degradation pathway. Polyester FPUFs tend to collapse more quickly, forming liquid tar rather than a solid char around the smoldering ignition source. Hence, the thermal degradation is shifted toward the non-oxidative decomposition pathway. As a result, polyester FPUFs smolder moderately and might not show sustained smoldering even when their cell morphology has been tuned to boost smoldering (i.e., small and fully open cell structure).

Reticulated foams are generally designed for filtration applications where a tight cell size distribution is a key performance parameter [28]. However, the reticulation process does not intrinsically induce a more homogeneous cell size. This has been confirmed here by comparing the relative standard deviation for the cell area (Σ) of reticulated FPUFs and standard FPUFs. Both show a similar relative standard deviation of about 5%. Thus, no significant difference is observed in terms of cell size heterogeneity between reticulated and non-reticulated polyether FPUFs.

The cell opening and rupture of the windows during foaming is a very complex problem [36] and is difficult to reproduce [19]. The air permeability in standard FPUFs varies between replicate foams but also between different locations in the same foam, for example due to core-to-surface temperature gradients in the foam during manufacturing (foaming is an exothermic process). For these reasons, the fully-open-cell structure of reticulated FPUFs should provide more consistent air permeability than a standard FPUF.

This is confirmed by the data in Table 1. The average relative standard deviations of Φ calculated for all reticulated (R) and non-reticulated (NR) foam types in Table 1 are about (3 ± 1)% and (10 ± 10)%, respectively.

The more consistent air permeability in reticulated foams is even more obvious when Φ is measured throughout an entire foam rather than at a few specific locations. The air permeabilities (as well as the cell size) of two large FPUFs manufactured on a production line, one reticulated (foam type 10) and the other non-reticulated (foam type 6), were measured throughout the large foams with 60 or more replicate measurements. The relative standard deviations were about 14% and 3% for foam type 6 and 10, respectively.

Variations in Φ might be particularly critical when $\Phi \approx \Phi_{\text{threshold}}$. In such a foam, there may well be locations where $\Phi > \Phi_{\text{threshold}}$ (sustained smoldering) and locations where $\Phi < \Phi_{\text{threshold}}$ (non-sustained smoldering). As a result, both sustained and non-sustained smoldering can be observed for foam samples from the same production run, and smoldering appears to be erratic. For example, for foam type 6 ($\Phi = (78 \pm 22)$ m min^{-1}) the probability that $\Phi < 78-2\sigma = 56$ m min$^{-1} \approx \Phi_{\text{threshold}}$ is about 5% (assuming a normal distribution of Φ), and this value is in qualitative agreement with the percentage of non-sustained smoldering observed experimentally (2 of 47 tests, i.e., about 4% of the tests) using samples from throughout the large foam. Foam type 10 has a value of CVF_{SM} comparable to foam type 6 but an air permeability $\Phi >> \Phi_{\text{threshold}}$, and non-sustained smoldering was never observed (6 tests).

Ideally, a reference foam requires a constant and homogeneous number of cell windows and cell size for consistent smoldering. In particular, the air permeability should be higher than $\Phi_{\text{threshold}}$ throughout the entire large foam to assure consistent sustained smoldering. Reticulated polyether FPUFs could be usefully exploited as reference foam materials. They show consistent values of permeability with $\Phi > \Phi_{\text{threshold}}$ throughout the entire foam, even at relatively small cell sizes (e.g., foam type 3). Their smoldering intensity can be easily tuned by adjusting the cell size to mimic the typical smoldering intensity observed in FPUFs commonly used for RUF. An increase in cell size can be simply obtained during foam production by increasing the pressure in the mixing head and keeping all other processing parameters constant [19].

The derivative of Eq. (1) with respect to Σ shows that $dCVF_{SM}/d\Sigma \propto \Sigma^{-3.8}$, thus the effect of cell size variations on CVF_{SM} drops sharply as Σ increases. This indicates that for a given target value of CVF_{SM}, a higher CVF_{SM} repeatability can be achieved by increasing the cell size and compensating the resulting reduction in CVF_{SM} with an increase in air permeability and/or the addition of a smoldering-promoter additive. For example, for a value of $CVF_{SM} \approx 20\%$, foam type 6 (smaller cell size) and foam type 10 (larger cell size, higher air permeability and carbon-black filled) have relative standard deviations of 47% and 20%, respectively. However, foam type 6 showed an exceptionally large variation in Φ and CVF_{SM}, but the variation in cell size was comparable to the other foam types. This suggests that, at least in foam type 6, the variations in air permeability played a major role in CVF_{SM} repeatability, and cell size variations were not as critical.

In the following section, it is shown how the repeatability of *CVF* measurements might be further improved by modifying the test setup.

3.2. Impact of the smoldering scenario: standard versus modified mockup test

The buoyant airflow is significantly suppressed in standard mockup tests, where a large fraction of the foam surface is in contact with the wooden frame that is not permeable to air (Fig. 1A). The modified mockup is redesigned to increase the surface area exposed to air and, thus, enhance the buoyant airflow (Fig. 1B).

In general, the foam thickness can also affect the airflow and, hence, smoldering by increasing the airflow resistance as it becomes thicker. For a rigorous sectional approach, the thickness of the foam mockups should be preferably characteristic of the foam thickness in the actual RUF (typically 10 cm or less). In this study, a foam thickness of 76 mm as previously specified in a proposed regulation [11], rather than 50 mm as recommended for standard mockups by other sources [12–14], has been used.

The char volume fractions in the standard mockup (CVF_{SM}) and modified mockup (CVF_{MM}) for foam types 3, 6 and 10 are reported in Table 2.

CVF_{MM} was always significantly higher than CVF_{SM}. For foam type 6 and 10, CVF_{SM} values were comparable (about 20%) and increase by a factor of 2.9 in the modified mockups for both foam types (i.e., $CVF_{MM}/CVF_{SM} \approx 2.9$). Noticeably, the cell size and air permeability were about double in foam type 10 as compared to type 6 (Table 1). This suggests that FPUFs with comparable CVF_{SM} show a comparable CVF_{MM}, independent of the value of air permeability and cell size of the foam.

The char volume fractions in foam type 3 ($CVF_{SM} \approx 69\%$ and $CVF_{MM} \approx 92\%$) were much higher than foam types 6 and 10. This means that most of the foam was already converted into char by the end of the test, and any remaining virgin foam was mainly localized on the corner edges of the foam mockup. In this situation, the rate of smoldering propagation during the 45 min test was reduced due to foam depletion, especially in the modified mockup. As a result, the ratio CVF_{MM}/CVF_{SM} was relatively low (about 1.3).

Table 2 also shows the values of relative standard deviation ($^{rel}\sigma$) for *CVF*. The values of $^{rel}\sigma$ were always less in the modified mockup (i.e., $^{rel}\sigma_{MM} < {}^{rel}\sigma_{SM}$). In other words, the repeatability of the test improved in the modified mockup. This was due, at least in part, to the fact that the value of $^{rel}\sigma$ tends to zero as *CVF* tends to 100%. This likely explains the low values of $^{rel}\sigma$ for foam type 3.

Noticeably, foam types 6 and 10 had comparable values of *CVF*, and the reticulated foam (i.e., foam type 6) had significantly lower values of $^{rel}\sigma$ in both the standard and modified mockups. This shows that reticulated foams tended to provide a more reproducible smoldering propagation rate in both test configurations.

The smoldering behavior of the two reticulated foams was further investigated with a slightly modified configuration: mockups were placed in enclosures to suppress air turbulence and promote a laminar buoyant airflow. Surprisingly, this apparently minor variation had major effects on smoldering. Transition to flaming (TTF) was never observed without the enclosure. When an enclosure was used, TTF occurred consistently (three tests) within 45 min in the modified mockup with foam type 3. With foam type 10, TTF might also occur at a later stage, but was not observed during the 45 min test (TTF occurred in one out of three tests at $t \approx 50$ min). Noticeably, TTF did not occur in the standard mockup.

Table 2
Char volume fraction (*CVF*) measured in the standard mockup (SM) and modified mockup (MM) for foam types 3, 6 and 10. The number of replicate tests in the modified mockup is five, and five or more in the standard mockup (see Table 1). Uncertainty is reported as two standard deviations (2σ).

	FPUF type 3 (reticulated)		FPUF type 6 (non-reticulated)		FPUF type 10 (reticulated)	
	Mockup type		Mockup type		Mockup type	
	SM	MM	SM	MM	SM	MM
CVF (%)	69 ± 12	92 ± 2	17 ± 16	49 ± 22	20 ± 8	58 ± 6
$2\,{}^{rel}\sigma$ (%)	18	2	94	44	40	10

$^{rel}\sigma$: relative standard deviation.

In the modified mockup, before achieving TTF, the air temperature (measured on the back of the wood frame) increased by at most 10 °C, and smoke completely filled the enclosure; such accumulation of combustible volatiles probably promoted TTF.

Temperature and mass loss data, recorded during these tests, are displayed in Figs. 4 and 5. In particular, Fig. 4A and B show the temperature profiles for thermocouples TC1 to TC5 measured in the standard mockup (*TC1S* to *TC5S*) and the modified mockup (*TC1M* to *TC5M*) with foam type 3. Fig. 4C shows the temperature differences ($DTC1 = TC1M - TC1S$) to ($DTC5 = TC5M - TC5S$) at a given time between the modified and the standard mockup with foam type 3. Fig. 4D shows the mass loss of the mockup (equal to the sum of the mass losses of the foam, fabric, cotton sheeting and cigarette) as a function of time with foam type 3. The same type of data are shown in Fig. 5 for foam type 10.

Temperatures slightly above 300 °C at a depth of about 3 cm have been shown to be sufficient to promote sustained smoldering in FPUF [20,27,37]. For this reason, the time to reach a temperature of 300 °C was used in this work as an indicator of the time to sustained smoldering. A temperature of 300 °C at a depth of about 4 cm was reached within 25 min in the standard mockup and 16 min in the modified mockup for foam type 3; 43 min in the standard mockup and 37 min in the modified mockup for foam type 10 (see TC3 temperature profiles in Figs. 4 and 5). Thus, not only the foam type, but also the test configuration played an important role on the time required to sustained smoldering. As a result, certain upholstery fabrics might lead to sustained FPUF smoldering only in the modified mockup (experimental data confirmed this hypothesis for a specific type of foam and cover fabric).

Figs. 4 and 5 show similar trends for both foam types, though type 3 smolders more readily. In the first 30 min, thermocouple TC3 (located closest to the ignition source) reached the highest temperature, followed by TC4, TC2, TC5 and TC1. This was true in both test configurations. In the last 5 min, the temperature ranking was $TC3S \approx TC2S > TC4S \geq TC1S > TC5S$ in the standard mockup, and $TC1M \geq TC2M > TC3M > TC4M > TC5M$ in the modified mockup. Thus, there was an obvious difference in temperature profiles between the two types of mockups. This can be clearly seen in Figs. 4C and 5C, where the differences between the measured temperatures in the modified and standard mockups (*DTC1* to *DTC5*) are plotted. Towards the end of the test ($t = 45$ min), *TC1M* was much higher than *TC1S* (DTC1 was about 400 °C with foam type 3 and 300 °C with type 10). Similarly, *TC2M* was higher than *TC2S* (*DTC2* by about 300 °C for foam type 3 and 120 °C for type 10). It appeared that the temperatures located near the bottom of the vertical foam (*TC1M*) rose much faster, when convective flow was not impeded by the presence of an air-impermeable wood substrate. This has important implications in terms of TTF and explains why TTF was observed only in the modified mockup.

For foam type 3, the temperature of the vertical foam close to the top (in proximity of TC5) at first showed a rapid increase (see Fig. 4) and then quickly dropped. Similar trends were also observed for TC4 and TC3, though to lesser extents, and are most evident in the modified mockup (see Fig. 4B). This might be explained as follows. During the propagation of the smoldering wave, the temperature was moderated in a range between 300 °C and 400 °C (the actual temperature depends on heat losses, airflow velocity and specific surface area of the foam) by the partial pyrolytic decomposition of the FPUF, and a highly porous char was produced. Once the smoldering front reached the bottom of the vertical foam (in proximity of TC1), oxygen was no longer depleted by the initial oxidation of foam to char and became largely available for the oxidation of the generated char. This char oxidation reaction created a second thermal wave that was more exothermic than the first wave (where the pyrolytic component was substantial), due to

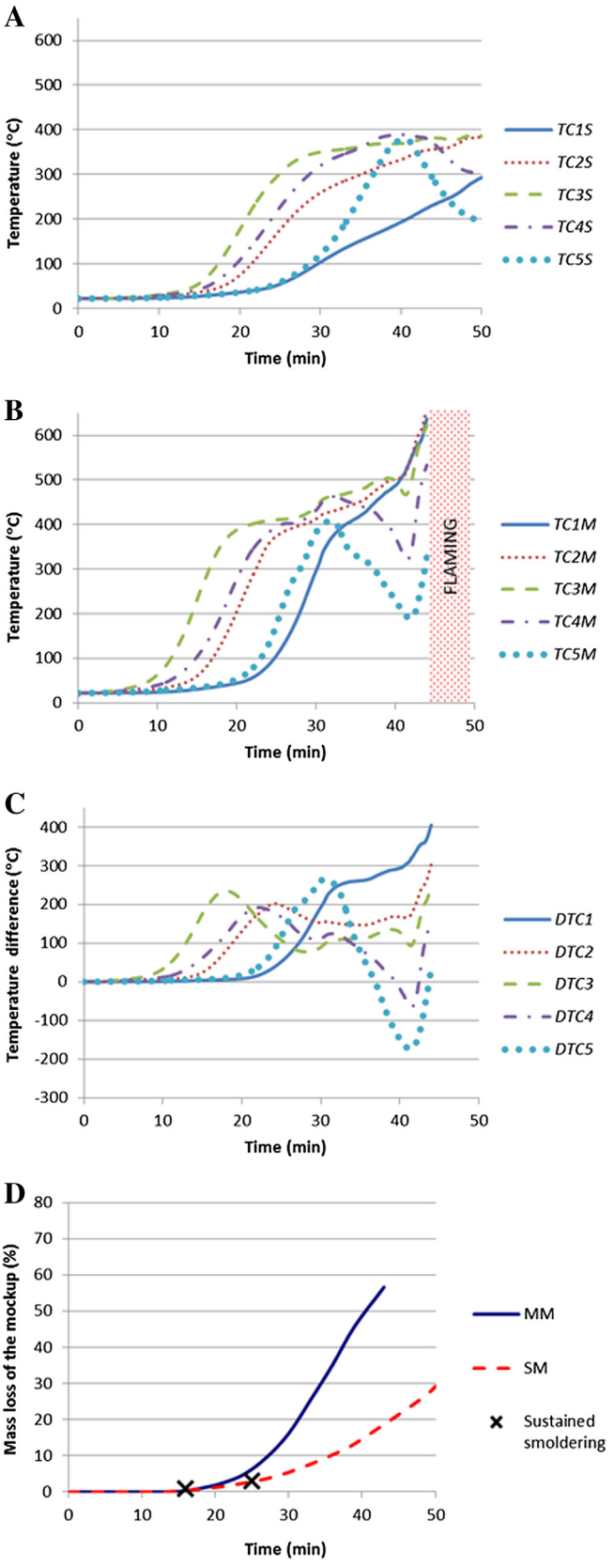

Fig. 4. Temperature profiles for thermocouples TC1 to TC5 (see Fig. 1) in the standard mockup test (A), in the modified mockup test (B), temperature difference between the two tests (C), and mass loss of the mockup (D) for foam type 3. The cross-shaped data points indicate the mass loss and time to reach 300 °C at TC3. TTF occurrence is labeled as "flaming" in Fig. 4B.

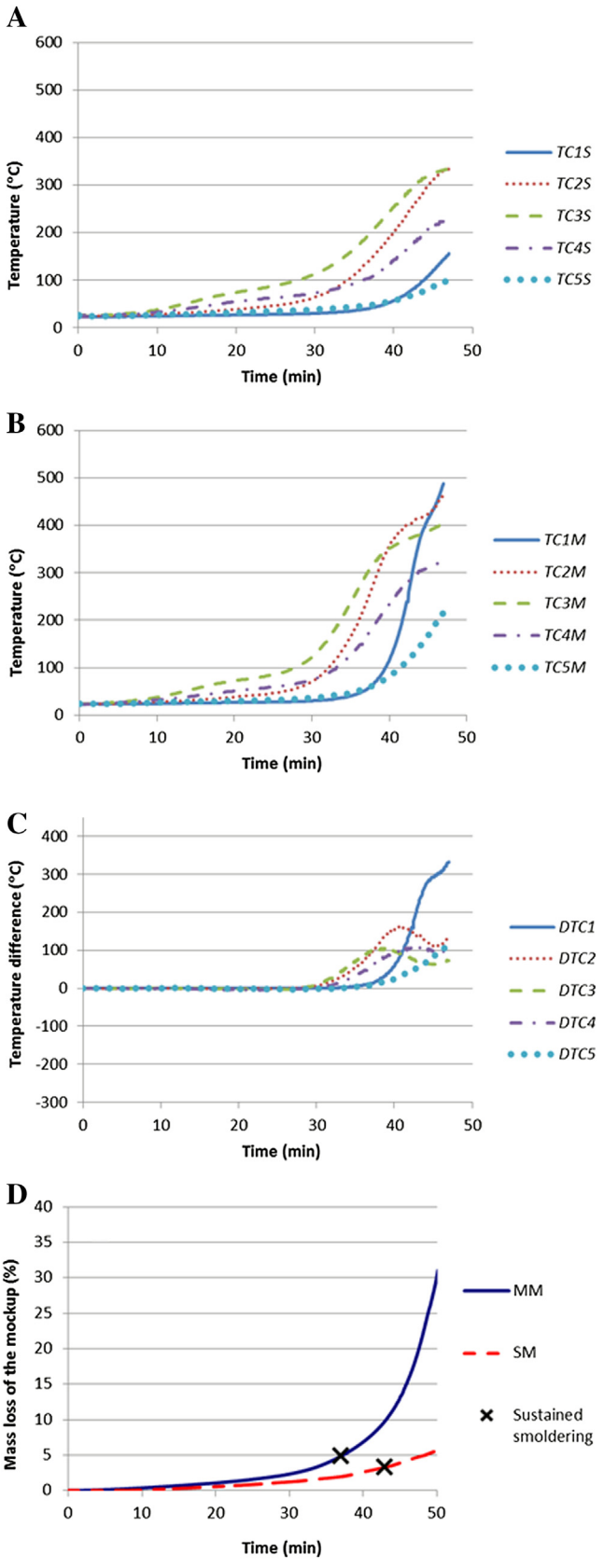

Fig. 5. Temperature profiles for thermocouples TC1 to TC5 (see Fig. 1) in the standard mockup test (A), in the modified mockup test (B), temperature difference between the two tests (C), and mass loss of the mockup (D) for foam type 10. The cross-shaped data points indicate the mass loss and time to reach 300 °C at TC3.

higher specific surface area that shifted the decomposition towards oxidative rather than pyrolytic decomposition (char has a specific surface area at least ten times higher than the virgin FPUF [20]). The second reaction wave moved back up (from TC1 to TC5), induced temperatures above 400 °C and eventually resulted in transition to flaming [22,23]. In the modified mockup, the intensity of this second wave was much higher than in the standard mockup presumably due to the presence of higher convective buoyant airflow. In this situation, the resulting high rate of char oxidation can rapidly deplete oxygen in the buoyant airflow and suppress the oxidative exothermic reactions in the upper sections of the foam/char (in proximity of TC5) [38]. As a result, the temperature in these regions can decrease (for example, see *TC5M* and *TC4M* in Fig. 4B for 32 min $< t <$ 42 min).

The sudden inversion in the temperature trend for *TC5M*, *TC4M* and *TC3M* at $t \approx 42$ min, observed in Fig. 4B, suggests an abrupt change of the smoldering scenario in proximity of these thermocouples. The resulting rapid temperature increase might be related to the propagation of the second oxidative wave sustained by a more vigorous buoyant airflow (the airflow increases with the temperature of the foam/char and the formation of large pores and cavities inside the foam/char [23,27,37]). The buoyant airflow is never perfectly vertical; there is always a horizontal component that moves air towards the low pressure field generated inside the foam/char. The horizontal component of this enhanced buoyant airflow might be sufficient to sustain the char oxidation in the upper regions of the foam. In addition, reactions in the gas-phase might also play an important role above 500 °C [23].

Noticeably, for foam type 10 (Fig. 5B), there is no drastic drop in *TC5M* by the time *TC1M* reaches 500 °C. Foam type 10 has a lower specific surface area (due to larger cell size) and higher air permeability compared to foam type 3. As discussed in Section 3.1, the resulting higher airflow velocity and lower rate of foam oxidation can result in: (a) thicker and lower-temperature smoldering wave for oxygen-limited smoldering, or (b) incomplete oxygen depletion in the buoyant airflow for kinetically-limited smoldering. In both cases, the temperature drop in *TC5M* for foam type 10 might be impeded.

Finally, Figs. 4D and 5D show the mass loss of the mockup as a function of time. There was at least a 3-fold increase in mass loss for both foam types when the modified mockup was used. The cross shaped data points in Figs. 4D and 5D indicate the times to reach a temperature of 300 °C at TC3 (used as an indicator of sustained smoldering) and the corresponding mass loss. Noticeably, the mass loss at the estimated times for sustained smoldering is extremely low. It ranged between about 1% (foam type 3) to 5% (foam type 10). Foam type 3 was expected to have a lower value, because its rate of smoldering propagation was higher, so less fabric was consumed by smoldering by the time that the 300 °C temperature limit was reached in the foam.

Currently, a *CVF* criterion (expressed as foam mass loss) [11] or a superficial charred length criterion [12–14] is used to assess smoldering behavior in standard mockup tests. *CVF* measurements are inconvenient (as they require the careful removal of the char at the end of the test) and are not a real-time measurement (a real-time measurement takes less time since a test can be interrupted once a prescribed limit is reached, e.g., a temperature value). The measurement of the charred length on the surface of the mockup does not distinguish between fabric-piloted smoldering without sustained foam smoldering, which is superficial, and a more severe foam-sustained smoldering, where the smoldering wave penetrates into the foam and no longer requires persistent smoldering of the upholstery fabric and/or barrier. Furthermore, continued smoldering can occur in the crevice between the vertical and horizontal cushions, while the cover fabric exhibits only a short char length [4]. Thus, smoldering assessment and early detection of

sustained smoldering in the mockup test might be more conveniently and effectively determined by measurements of the foam temperature (e.g., TC3), rather than measurements of superficial-smoldering length or mass loss as currently prescribed in standard smoldering tests.

4. Conclusions

This work aims to provide guidance for the selection of reference FPUF for smoldering tests and the development of a bench-scale smoldering test able to identify the combinations of upholstery materials that will likely prevent self-sustained smoldering in actual furniture.

In the first part of this study, the effect of foam morphology was discussed. It was shown that cell size is a surprisingly robust predictor of the rate of smoldering propagation for polyether FPUFs that do not contain additives (such as inorganic fillers or flame retardants) and have sufficiently high values of air permeability (values usually observed in commercial RUF foams). There is a threshold value of air permeability below which sustained smoldering does not occur. Local variations in the fraction of open-to-closed cells in a polyether FPUF may not significantly affect smoldering in foams where the air permeability is consistently higher or lower than the threshold value, but may induce erratic smoldering behavior in foams having an average air permeability close to the threshold value. Reticulated FPUFs, possibly filled with carbon black, should prove useful as reference FPUFs. The reticulation process improves the smoldering repeatability by minimizing the variability of air permeability throughout the foam. For reticulated polyether FPUFs, smoldering intensity can be easily tuned by adjusting the cell size to mimic the typical smoldering intensity observed in FPUFs for RUF. Reticulated polyester FPUFs have a very uniform cell structure, but should not be used as reference materials due to limited smoldering even for extremely small cell sizes.

In the second part of the paper, it was shown how a variation in the design of the bench-scale test apparatus had a major effect on smoldering behavior. Due to surface blockage of the foam, it is expected that the standard mockup test significantly suppresses buoyancy-induced natural convection and oxygen supply within the foam. As a result, the rate of smoldering propagation is reduced. For this reason, the standard mockup test might underestimate smoldering in those types of RUFs where the buoyant airflow within the foam is not hindered. The modified mockup test was designed to mimic this smoldering scenario. Up to a 3-fold increase in the rate of smoldering propagation and a 400 °C increase in smoldering temperature was observed in the modified test as compared to the standard test. The time to sustained smoldering decreased, and the repeatability of the test, in terms of charred volume fraction, improved in the modified mockup. Transition to flaming was achieved in the modified mockup only when an external enclosure was used. In summary, the modified mockup has proven to be a more severe test than the standard mockup. It may offer a near-worst-case scenario, useful to identify the upholstery materials that will most likely prevent smoldering ignition in actual furniture independently of its configuration or geometry.

Finally, it was demonstrated that FPUF smoldering assessment and early detection of sustained smoldering might be conveniently and effectively achieved by measurements of the foam temperature, rather than measurements of superficial smoldering length or mass loss, as currently prescribed.

Acknowledgments

The Consumer Product Safety Commission (CPSC) is acknowledged for financial and technical support. The authors are grateful to J. R. Shields, R. G. Gann and A. Hamins (NIST) for their contributions.

References

[1] Ahrens M. Home structure fires that began with upholstered furniture. Quincy, MA: National Fire Protection Association; 2011.
[2] Hall Jr JR. The other way cigarettes kill. Natl Fire Prot Asssoc J 1998;92:56–63.
[3] Evart B. Home fires that began with matresses and bedding. Quincy, MA: National Fire Protecion Association; 2011.
[4] Babrauskas V, Krasny J. NBS monograph 173-fire behaviour of upholstered furniture. Gaithersburg, MD: National Institute of Standards and Technology, National Engineering Laboratory, Center for Fire Research; 1985. Available on Oct. 2 2013 from: www.bhfti.ca.gov/about/laws/attach_2.pdf.
[5] 16 CFR 1632-standard for the flammability of mattresses and mattress pads (FF 4-72, AMENDED). U.S. Consumer Product Safety Commission; 2012.
[6] 16 CFR 1633-standard for the flammability (open flame) of mattress sets (71 FR 13498). U.S. Consumer Product Safety Commission; 2012.
[7] Nazare S, Davis R. A review of fire blocking technologies for soft furnishings. Fire Sci Rev 2012;1:1.
[8] Nazaré S, Davis R, Butler K. Assessment of factors affecting fire performance of mattresses: a review. Fire Sci Rev 2012;1:1–27.
[9] Gann RG. The challenge of realizing low flammability home furnishing. In: 13th international fire science and engineering conference. London: Interscience Communications; 2013.
[10] Babrauskas V. Capabilities and limitations of fire barriers. In: Upholstered furniture fire safety technology meeting: part 3-July 10, 2013. U.S. Consumer Product Safety Commision; 2013. Available on Oct. 2 2013 from: www.cpsc.gov/Newsroom/Multimedia/?vid=64503.
[11] Standard for the flammability of residential upholstered furniture; proposed rule (73 FR 11702). U.S. Consumer Product Safety Commision; 2008.
[12] ASTM. Standard E1353, standard test methods for cigarette ignition resistance of components of upholstered furniture; 2008. West Conshohocken, PA.
[13] Requirements, test procedure and apparatus for testing the flame and smolder resistance of upholstered furniture. State of California: Department of Consumer Affairs, Bureau of Home Furnishings and Thermal Insulation; 2013.
[14] Filling/padding component test method–barrier test method–fabric classification test method. Upholstered Furniture Action Council (UFAC); 1990.
[15] Gann RG, Hnetkovsky EJ. NIST TN 1627-modification of ASTM E 2187 for measuring the ignition propensity of conventional cigarettes. National Institute of Standards and Technology; 2009.
[16] Upholstered furniture memoranda. Bethesda, MD: U.S. Consumer Product Safety Commission; 2012. Available on Oct. 2 2013 from: www.cpsc.gov/PageFiles/129840/ufmemos.pdf.
[17] Toner HP. Ignition of foam/fabric composites in residential upholstered furniture. J Consumer Prod Flammabl 1982:85–94.
[18] Zammarano M, Matko S, Krämer RH, Davis RD, Gilman JW, Sung LP, et al. Smoldering in flexible polyurethane foams: the effect of foam morphology. In: Fire and polymers VI: new advances in flame retardant chemistry and science. American Chemical Society; 2012. pp. 459–79.
[19] Zammarano M, Krämer RH, Matko S, Mehta S, Gilman JW, Davis RD. NIST TN 1747–factors influencing the smoldering performance of polyurethane foam; 2012.
[20] Rogers FE, Ohlemiller T. Smolder characteristic of flexible polyurethane foams. J Fire Flamm 1980;11:32–44.
[21] Ravey M, Pearce EM. Flexible polyurethane foam. I. Thermal decomposition of a polyether-based, water-blown commercial type of flexible polyurethane foam. J Appl Polym Sci 1997;63:47–74.
[22] Aldushin AP, Bayliss A, Matkowsky BJ. On the transition from smoldering to flaming. Combust Flame 2006;145:579–606.
[23] Dodd AB, Lautenberger C, Fernandez-Pello C. Computational modeling of smolder combustion and spontaneous transition to flaming. Combust Flame 2012;159:448–61.
[24] Torero JL, Fernandez-Pello AC. Natural convection smolder of polyurethane foam, upward propagation. Fire Saf J 1995;24:35–52.
[25] Ohlemiller TJ, Bellan J, Rogers F. A model of smoldering combustion applied to flexible polyurethane foams. Combust Flame 1979;36:197–215.
[26] Nield DA, Bejan A. Convection in porous media. New York: Springer; 2012.
[27] Salig RJ. The smoldering behavior of upholstered polyurethane cushionings and its relevance to home furnishing fires. Thesis (M.S.). Cambridge, MA: Massachusetts Institute of Technology; 1982.
[28] Eaves D. Handbook of polymer foams. Shawbury: Rapra Technology; 2004.
[29] Kino GS, CT R. Confocal scanning optical microscopy and related imaging systems. Academic Press; 1996.
[30] Schneider CA, Rasband WS, Eliceiri KW. NIH image to ImageJ: 25 years of image analysis. Nat Meth 2012;9:671–5.
[31] Gummaraju RV, Pask RF, Koller HJ, Wujcik SE, Reimann KA. Evaluation, modification and adaptation of an airflow test method for polyurethane foams. J Cell Plastics 2001;37:193–206.
[32] Oh C, Kim E, Lim J, Schultz R, Petti D. Effect of reacting surface density on the overall graphite oxidation rate. In: International congress on advances in nuclear power plants 2009 Tokyo, Japan 2009. pp. 206–12.

[33] Leach SV, Ellzey JL, Ezekoye OA. Convection, pyrolysis, and Damköhler number effects on extinction of reverse smoldering combustion. Symposium Int Combust 1998;27:2873–80.
[34] Leach SV, Rein G, Ellzey JL, Ezekoye OA, Torero JL. Kinetic and fuel property effects on forward smoldering combustion. Combust Flame 2000;120:346–58.
[35] Landers R, Hubel R, Borgogelli R. The importance of cell structure for viscoelastic foams. PU Mag 2008;1:40–7.
[36] Zhang XD, Davis HT, Macosko CW. A new cell opening mechanism in flexible polyurethane foam. J Cell Plastics 1999;35:458–76.
[37] Anderson MK, Sleight RT, Torero JL. Downward smolder of polyurethane foam: ignition signatures. Fire Saf J 2000;35:131–47.
[38] Rein G, Carlos Fernandez-Pello A, Urban DL. Computational model of forward and opposed smoldering combustion in microgravity. Proc Combust Inst 2007;31:2677–84.